MEDDOCS Open Access Publisher

Journal of Nanomedicine

Open Access | Review Article

Yolk-shell structure for upconverting nanoparticles: Bioimaging, drug delivery, and photodynamic therapy

***Corresponding Author(s): Ilkeun Lee,**

Department of Chemistry, University of California, Riverside, USA

Tel: +1 (951) 827-5736; Fax: +1 (951) 827-4713

Email: ilkeun@ucr.edu

Received: Jan 04, 2018

Accepted: Jan 26, 2018

Published Online: Feb 14, 2018

Journal: Journal of Nanomedicine

Publisher: MedDocs Publishers LLC

Online edition: http://meddocsonline.org/

Keywords: Upconverting Nanoparticles (UCNP); Yolk-shell; Bioimaging; Drug delivery; Photodynamic therapy; Theranostics

Graphical Abstract

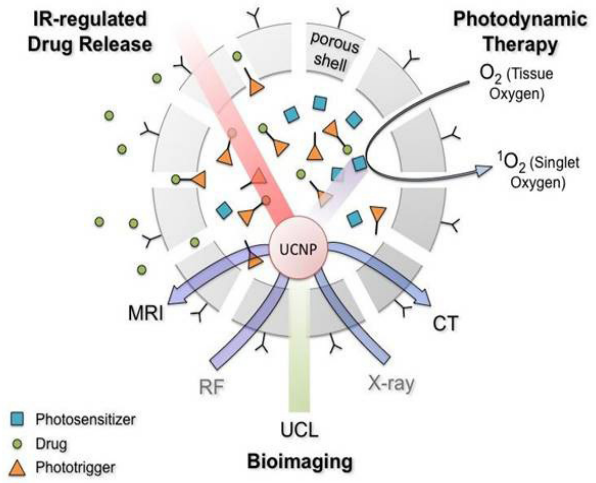

Abstract

Upconverting Nanoparticle (UCNP) has recently received many attentions from theranostics and nanomedicine fields because it can be designed for multi-functional targeted nanomedicines with multi-modal imaging. One of popular UCNPs is $NaLnF_4$: Yb,Er/Tm, which absorbs infrared and releases visible or ultraviolet light to trigger drug release or to produce singlet oxygen for therapy. Lantanides doping enhances upconversion luminescence and enable magnetic resonance imaging. In addition IR-regulating drug release reaches deep without harm. Core-shell nanostructures have been applied for the most of UCNP applications, but the therapeutic efficacy is still far away from the desired levels in nanomedicine. First, loading space is limited by the thickness or porosity of shell, so enough loading isn't guaranteed in most of core-shell structures. Thicker shell is better for higher loading, but a bigger particle size is unavoidable. Porosity isn't a parameter to control simply. Second, only outer shell surface is offered for surface modifications to specific binding or properties, which is critical of targeted therapy. However, when UCNP is housed in a yolk-shell structure, the void, which isn't available in core-shell structures, can be a solution for loading both drugs and photo triggers in drug delivery, or photosensitizers in photodynamic therapy. In addition, both inner and outer surfaces can be modified as any desired purposes. Third, the movable yolk UCNP has more chance to contact with photo triggers and photosensitizers in the void. All the benefits with yolk-shell structure are resulted in high therapeutic efficacy. In this mini review, some of yolk-shell UCNP examples are introduced for in vivo multimodal bioimaging with high contrast, IR-regulated drug release, and high efficacy in photodynamic therapy.

Introduction

"Theranostics" is a term that combines therapy with diagnosis, and a medicine field that therapy and diagnosis occur together at the same target [1]. It can't be accomplished without very specific targeting ability in diagnosis, high contrast agents in bioimaging, enough amount and simple release in drug delivery, and high efficacy in therapy. Recently upconverting nanoparticle (UCNP) has been one of promising platforms, where

Cite this article: Lee I. Yolk-shell structure for upconverting nanoparticles: Bioimaging, drug delivery, and photodynamic therapy. J Nanomed. 2018; 1(1): 1004.

nanomedicine meets theranostics and improves its therapeutic level. UCNPs exhibit the photon upconversion that convert two incident lower energy photons to one higher energy photon [2]. They are commonly composed of lanthanide or actinide-doped transition metals, because they have multiple 4f electrons with long enough excitations for upconversion [2]. In biomedical applications, one of popular UCNPs is $NaLnF_4$:Yb,Er/Tm [3,4]. Yt-terbium-erbium or ytterbium-thulium are sensitizers and doped to $NaLnF_4$ nanoparticles for absorbing infrared (IR) and releasing visible (Vis) or ultraviolet (UV) light [2,5,6]. Sodium (Na^+) is a cation with a similar radius, while fluoride (F^-) has a low phonon energy with a good stability. Their synthesis has been already reviewed in many literatures [1,4,7]. For the practical applications such as water soluble or binding to functional groups, core UCNPs need to be coated with inorganic materials or capping polymers [8,9]. UCNP@silica core-shell nanostructure is one of popular forms because of easy preparation [10], water-soluble, and biocompatible features. Titania, [11] drug-conjugated, [12] and capping ligands [13] are also available for the shell materials. No matter what the material is, the main challenge would be the loading ability to deliver drugs, photo triggers, or photosensitizers to targets. The therapeutic efficacy with core-shell nanostructures is limited by the loading space in the shell. Porosity or pore size distribution couldn't be adjusted simply from the synthetic procedures. Simply thicker shell or larger dose is required for higher loading, but a bigger particle size or any side effect caused by heavy doses would be inevitable.

Yolk-shell structure is so-called "rattle" representing yolk@void@shell configuration [14-16] and has more benefits than core-shell structure. First, the void can be filled with anything to deliver or carry. It is a much larger amount than any loading in core-shell structures. Second, both inner and outer surfaces can be modified as desired (e.g. one is hydrophobic, the other is hydrophilic). It is quite useful when keeping undesired chemicals inside of the shell, but releasing drugs only to outside targets. Core-shell has an option at outer surface only. Third, yolk is movable and can have more chance of contact with anything in void. For the applications in nanomedicine, UCNP is commonly placed at yolk position, and mesoporous silica has been one of frequent materials for shell. Photo trigger-conjugated drug or photosensitize can be stored in both void and pores of shell, which are better than only pores of core-shell structure. In addition, much higher energy transfer efficiency in photodynamic therapy is available with movable UCNP yolk. Both inner and outer surfaces of shell are modified with desired surface properties, or tethered to any specific binding to tumor or cancer cell surfaces. When UCNPs meet yolk-shell nanostructure, theranostics can be achieved as multimodal imaging, target specificity, and multifunctional therapeutic properties.

Radiotherapy and chemotherapy have been widely used in cancer treatments [17,18]. However, radiotherapy fails to eradicate hypoxic tumors and high doses of irradiation unavoidably because damage to normal cells [19]. Chemotherapy is limited for drug resistant cells [20]. Its efficacy may be improved by high doses, but side effects would cause other diseases. Although both therapies destroy cancer DNA structures, the DNA can self-repair to reproduction and regrowth. In photodynamic therapy, [21,22] cytotoxic singlet oxygen ($^1O_2$) can be more efficient at killing cancer cells, as it inhibits DNA repair and elicits to cell death. UCNPs convert NIR to Vis or UV light, and continuous wave near-infrared (CW NIR) is the ideal excitation source for photosensitizer to generate singlet oxygen. In addition, NIR lights penetrate deeply into tissues with no harm.

In this mini review, only some of selected UCNP examples built in yolk-shell nanostructures are introduced to prospect for practical applications in nanomedicine. In vivo tri-modal bioimaging is available with upconversion luminescence (UCL), magnetic resonance imaging (MRI), and computed tomography (CT) [23]. Chlorambuchil drug release is regulated by IR light and amino-coumarin phototrigger [24]. High efficacy in photodynamic therapy using singlet oxygen ($^1O_2$) is obtained from $NaLuF_4$:Gd/Yb/Er encapsulated in amino-terminated organ silica shell when both IR and photosensitize are present [25].

Bioimaging

Various technologies using ultrasonic, optical, luminescent, magnetic, or X-ray sources are available for bioimaging. The main requirements in nanomedicine include spatial resolution, sensitivity to tumor/cancer cells, penetration depth, etc. Recently rare-earth UCNPs have being considered as promising fluorescent imaging probes [26]. UCL imaging has a deeper penetration depth with NIR than conventional photoluminescence using organic dyes/quantum dots and UV light. In addition, neither harm nor auto fluorescence in bioimaging. MRI has a much deeper penetration depth and a much better contrast. If magnetization recovers before MR measurement, the image weighting is denoted by T_1. If it decays before the measurement, that is denoted by T_2. Tumor signal is high in T_2-weighted, but low in T_1-weighted MR images [27]. CT images are preferred when high special resolution is required [28].

In UCNPs, Gd^{3+} doping enhances UCL [29,30] and allows application as a contrast agent for in vivo MRI [31]. Hence magnetic/luminescent dual-mode imaging is available with Gd-doped UCNPs. **Figure 1** shows one of examples [32]. UCNP is $NaYF_4$:Yb/Er, and additionally Gd is doped via seed-mediated process for Gd-UCNP ($NaYF_4$:Yb/Er@$NaGdF_4$). UCSN is the final yolk-shell structure in **Figures 1A**. A nude mouse bearing HeLa tumor was used for bioimaging experiments, and MR (**Figures 1B,C**) and UCL (**Figures 1E**) images were measured before and after the intratumoral injection of UCSN as contrast agents in vivo. High signal intensity at the tumor site indicates not only targeting folate receptors in HeLa tumor cells [33], but also enhanced MRI. In addition, in vivo UCL signal were also observed under a CW NIR laser (980 nm), demonstrating dual-mode (MR/UCL) imaging of UCSN in vivo.

Trimodal (UCL/MRI/CT) imaging is also possible. Zhu et al. [23] reported Yb^{3+} and Er^{3+}/Tm^{3+} co-doping to $NaLuF_4$. Fe_3O_4 nanoparticles are yolks for the magnetic manipulation without shielding UCL signal. HF/NaF solution converts Fe_3O_4@SiO_2@Lu_2O_3 core-double shell nanostructure to multifunctional Fe_3O_4@$NaLuF_4$:Yb,Er/Tm yolk-shell UCNP. After intratumoral injection of UCNPs, in vivo UCL images were measured in bright and dark fields. Excitation source is CW NIR at 980 nm, while 800 nm signal is measured with a high contrast. In vivo T_2-weighted MR and CT images were also obtained. After the injection, about 50% weaker (darker) signal was observed in the tumor area, demonstrating UCNPs as a good MRI contrast agent. High contrast of tumor area was also observed well in volume-rendered and coronal CT images. Volume rendering is a computer technique to get a 2-D projection of a 3-D sample. Trimodal imaging is applicable with yolk-shell structured UCNPs, although further research is required for smaller particle sizes, better sensitivity and deeper penetration depth.

Drug Delivery

Drug release can be triggered by photolysis, [34] pH responses, [35,36] redox, [37] enzymes [38] or temperature [39]. Among them, NIR light trigger using UCNPs has been succeeded in drug delivery with convenient manipulation and improved therapeutic efficacy. Traditional photo-regulated drug release uses UV light, which has a shorter penetration depth and is harmful to living tissues. In contrast to UV, CW NIR light penetrate deeper without damage [3]. Yb^{3+} and Tm^{3+} doped lanthanide upconversion nanoparticles convert CW 980 nm to UV light that drives photolysis to release drugs.

Zhao et al. [24] reported a photo-triggered drug release as shown in **Figure 2**. Yolk is $NaYF_4$:Tm,Yb@$NaLuF_4$, which convert NIR to intense UV emission, and shell is mesoporous silica that has a large pore volume to be loaded with hydrophobized phototrigger-conjugated drug (**Figure 2A,B**). Lipase is blocked by the mesoporous shell, hence enzymolysis is not allowed in yolk-shell nanostructures. Amino-coumarin is the phototrigger that releases chlorambuchil (an anticancer drug, denoted as ACCh) upon photolysis under UV adsorption at 380 nm. The phototrigger has hydrophobic two octanyl chains, which prevent from being released together with the drug. Drug release from the YSUCNP-ACCh was carried out in phosphate buffered saline (PBS, pH 7.5) solution. **Figure 2C** displays the drug release under CW NIR at 980 nm as a function of irradiation time. For the comparison, YSLnNP-ACCh, in which the yolk is $NaYF_4$:Yb@$NaLuF_4$ without Tm^{3+}, was also tested. Only YSUCNP-ACCh released the drug up to about 68%, while YSLnNP-ACCh did nothing due to the absence of Tm^{3+}. In addition, chlorambucil drug is released only when CW NIR laser is on (**Figure 2D**). Without light, the drug release stops. Kunming mice bearing S-180 tumor were used for photo-regulated drug delivery experiments. **Figure 2E** shows the photos of the mice injected with YSUCNP-ACCh, YSLnNP-ACCh or saline on 1st, 9th, and 17th day of NIR irradiation (980 nm, 50 mW/cm^2, 20 min each day). No big difference was observed in tumor volume for YSLnNP-ACCh and saline. In case of YSUCNP-ACCh, however, the tumor grew much slower, demonstrating successful drug release regulated by NIR light only.

Photodynamic Therapy

UCNPs can be applied for photodynamic therapy using photosensitizers under NIR light to produce cytotoxic singlet oxygen ($^1O_2$) that treat tumor cells in both in vivo and vitro. One of challenges for practical use is the efficacy of PDT, which depends on the efficiency of energy transfer from UCNPs to photosensitizers. Recently many core-shell typed UCNPs [21,22] have been developed for PDT, but sufficient photosensitizer loading adjacent to UCNPs prefers yolk-shell to core-shell nanostructures. Lu et al. [25] reported multifunctional nano-bioprobes based on organosilica-shelled UCNP as depicted in **Figure 3**. UCNP is b-$NaLuF_4$:Gd/Yb/Er capsulated in amino-terminated organosilica shell (ROS-ATF), which has a high affinity to urokinase plasminogen activator receptor (uPAR) as shown in **Figure 3A**. Mono-substituted b-carboxylphthalocyanine zinc (ZnPc-COOH) was used for a photosensitizer, as its absorption bands overlap with the red emission of Er^{3+}. The mesoporous ROS-ATF shell accommodate the photosensitizer as high as 7.7 wt.%. H1299 (human lung cancer) cells were used to evaluate in vitro PDT efficacy. **Figure 3B** displays the viability of H1299 treated with UCNP@ROS-ZnPc-COOH or UCNP@ROS as a function of concentration under NIR irradiation (980 nm, 0.5 W/cm^2, 10 min). The viability of H1299 by use of MTT assay decreased only when both NIR light and photosensitizer are present. The corresponding microscopic images before and after PDT treatment are in **Figures 3D,E**. For in intro cytotoxicity, HELF (human embryonic lung fibroblast) cells were incubated with UCNP@ROS-ZnPc-COOH for 12 and 24 h (**Figure 3C**). Decrease in HELF viability is just less than 20% even after 24 h at 0.1 mg/mL of concentration, indicating biocompatible. They also measured UCL lifetimes of $^4F_{9/2}$ at 654 nm for UCNP@ROS (rattle-structured organosilica), UCNP@OS (organosilica) and UCNP@RS (rattle-structured silica) with and without ZnPC-COOH loading to verify the energy transfer from UCNP to ZnPc-COOH (**Figure 4**). The lifetime decreased about a half after loading ZnPc-COOH to UCNP@ROS, while the decrease was about 5% with UCNP@RS. All the results match to the trends in the corresponding UCL spectra. The peak at around 660 nm almost disappeared with UCNP@ROS-ZnPc-COOH, indicating 98% of energy transfer efficiency. For comparison, 66% and 40% of efficiency were obtained for UCNP@OS-ZnPc-COOH and UCNP@RS-ZnPc-COOH, respectively.

Future Outlook

Multi-modal imaging and multi-functional therapy are fundamentals of theranostics. UCNPs in yolk-shell nanostructures have many advantages than core-shell, and already opened the door of nanomedicine wider as a successful platform for theranostics, but their preparation steps are usually not simple as one-pot synthesis. During the synthetic procedures, broken or no shell could be included. It may cause any undesired effect on normal cells. Actually yolk-shell nanostructure is already well known in heterogeneous catalysis. Damaged or deficient yolk-shell catalysts may drop the performance of catalysts, but not a safety issue. In medical application, however, it could be an important problem, as the bio safety of UCNPs [40,41] Further research should focus on simpler synthetic procedure for safer namomaterials.

Figures

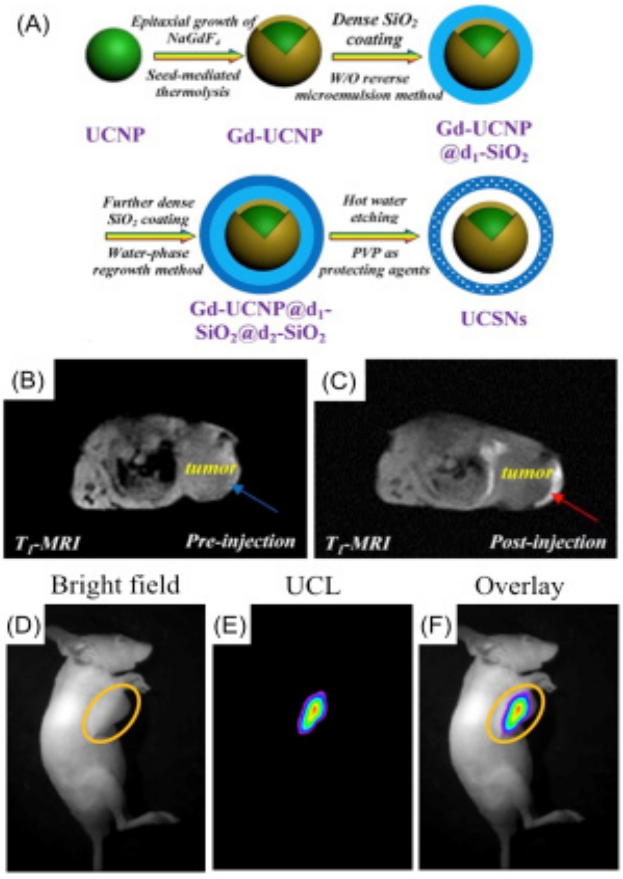

Figure 1: (A) Schematic diagram of UCNP synthesis, In vivo T1-MR images (B) before and (C) after intratumoral injection of UCNP@void@SiO_2, (D) Bright field and (E) in vivo upconversion luminescent image (UCL) after intratumoral injection of UCNP@void@SiO_2, (F) Overlay image of (D) and (E). Reproduced with permission from ref. [32]

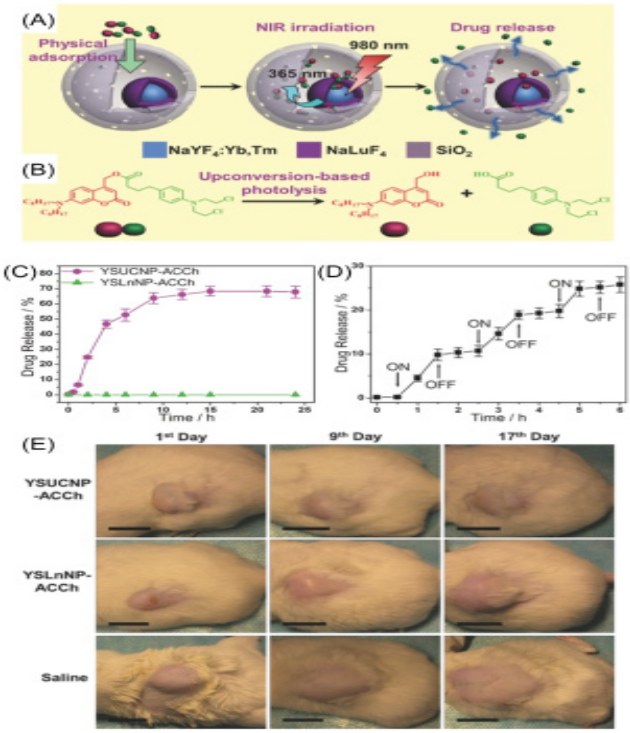

Figure 2: (A) Schematic diagram of drug delivery, (B) Upconversion-based photolysis, (C) Drug release profiles of chlorambucil from YSUCNP-ACCh and YSLnNP-ACCh in phosphate buffered saline solution (pH = 7.5) under CW 980 nm irradiation, (D) Release of chlorambucil drug from YSUCNP-ACCh as a function of 980 nm laser on and off, (E) Photos of tumor-bearing mice, to which are injected with YSUCNP-ACCh, YSLnNP-ACCh, or saline after NIR radiation treatments on the 1st, 9th and 17th day. Reproduced with permission from ref. [24]

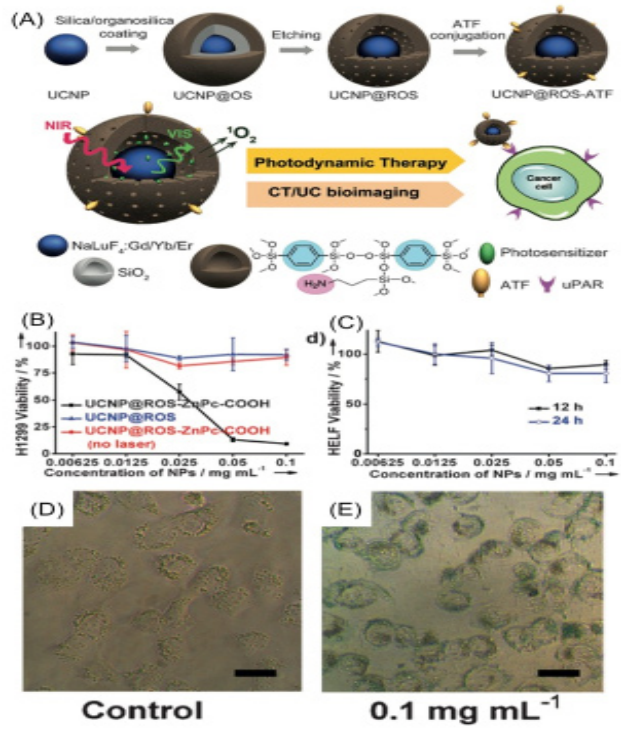

Figure 3: (A) Schematic illustration of amino-terminated organosilica-shelled UCNP (UCNP@ROS-ATF, noted for Rattle OrganoSilica-Amino Terminal Fragment), Viability of (B) H1299 and (C) HELF cells treated with UCNP@ROS-ZnPc-COOH and UCNP@ROS as a function of concentration with and without 980 nm irradiation, (D) and (E) Microscopic images of H1299 cells before and after photodynamic therapy treatment, respectively (scale bar = 25 μm). Reproduced with permission from ref. [25].

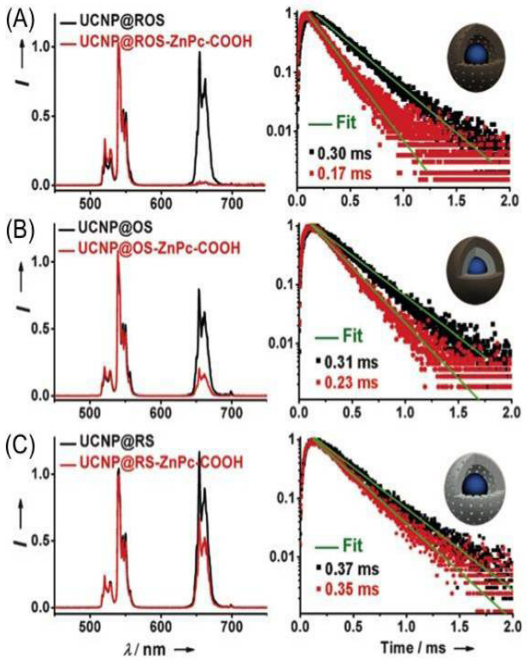

Figure 4: Upconversion luminescent spectra and lifetime of 4F9/2 for (A) UCNP@ROS, (B) UCNP@OS and (C) UCNP@RS with and without loading ZnPc-COOH. Reproduced with permission from ref. [25].

Acknowledgements

Ilkeun Lee thanks Junghyun Hong for helpful discussion.

References

1. Chen G, Qiu H, Prasad PN, et al. Upconversion nanoparticles: Design, nanochemistry, and applications in theranostics. Chem Rev. 2014; 114: 5161-5214.
2. Auzel F. Upconversion and anti-stokes process with f and d ions in solids. Chem Rev. 2004; 104: 139-173.
3. Idris NM, Jayakumar MKG, Bansal A, et al. Upconversion nanoparticles as versatile light nanotransducers for photoactivation application. Chem Soc Rev. 2015; 44: 1449-1478.
4. Wang M, Abbineni G, Clevenger A, et al. Upconversion nanoparticles: Synthesis, surface modification and biological applications. Nanomedicine: NBM. 2011; 7: 710-729.
5. Menyuk N, Dwight K, Pierce JW. NaYF4:Yb,Er-An efficient upconversion phosphor. Appl Phys Lett. 1972; 21: 159-161.
6. Liu X, Dng R, Zhang Y, et al. Probing the nature of upconversion nanocrystals: Instrumentation matters. Chem Soc Rev. 2015; 44: 1479-1508.
7. Kang D, Song X, Xing J. Synthesis and characterization of upconversion nanoparticles with shell structure and ligand-free hydrophilic modification. RSC Adv. 2015; 5: 83149-83154.

8. Sedlmeier A, Gorris HH. Surface modification and characterization of photon-upconverting nanoparticles for bioanalytical applications. Chem Soc Rev. 2015; 44: 1526-1560.

9. Wang F, Banerjee D, Liu Y, et al. Upconversion nanoparticles in biological labeling, imaging, and therapy. Analyst. 2010; 135: 1839-1854.

10. Chen X, Peng D, Ju Q, et al. Photon upconversion in core-shell nanoparticles. Chem Soc Rev. 2015; 44: 1318-1330.

11. Idris NM, Lucky SS, Li Z, et al. Photoactivation of core-shell titania coated upconversion nanoparticles and their effect on cell death. J Mater Chem B. 2014; 2: 7017- 7026.

12. Yang D, Dai Y, Liu J, et al. Ultra-small BaGdF5-based upconversion nanoparticles as drug carriers and multimodal imaging probes. Biomaterials. 2014; 35: 2011-2023.

13. Hu P, Wu X, Hu S, et al. Enhanced upconversion luminescence through core/shell structures and its application for detecting organic dyes in opaque fishes. Photochem Photobiol Sci. 2016; 15: 260-265.

14. Liu J, Qiao SZ, Chen JS, et al. Yolk/shell nanoparticles: New platforms for nanoreactors, drug delivery and lithium-ion batteries. Chem Commun. 2011; 47: 12578-12591.

15. Lee I, Joo JB, Yin Y, et al. A yolk@shell nanoarchitecture for Au/TiO_2 catalysts. Angew Chem Int Edit. 2011; 50: 10208-10211.

16. Purbia R, Paria S. Yolk/shell nanoparticles: Classifications, synthesis, properties, and applications. Nanoscale. 2015; 7: 19789-19873.

17. Mitrasinovic PM, Mihajlovic ML. Recent advances in radiation therapy of cancer cells: a step towards an experimental and systems biology framework. Curr Radiopharm. 2008; 1: 22-29.

18. Allen TM, Cullis PR. Drug delivery systems: Entering the mainstream, Science. 2004; 303: 1818-1822.

19. Nakae T, Uto Y, Tanaka M, et al. Design, synthesis, and radiosensitizing activities of sugar-hybrid hypoxic cell radiosensitizers. Bioorgan Med Chem. 2008; 16: 675-682.

20. Szakacs G, Paterson JK, Ludwig JA, et al. Targeting multidrug resistance in cancer. Nat Rev Drug Discov. 2006; 5: 219-234.

21. Idris NM, Gnanasammandhan MK, Zhang J, et al. In vivo photodynamic therapy using upconversion nanoparticles as remote-controlled nanotransducers. Nat Med. 2012; 18: 1580-1585.

22. Wang C, Tao H, Cheng L, et al. Near-infrared light induced in vivo photodynamic therapy of cancer based on upconversion nanoparticles. Biomaterials. 2011; 32: 6145-6154.

23. Zhu X, Zhou J, Chen M, et al. Core-shell Fe_3O_4@$NaLuF_4$:Yb,Er/Tm nanostructure for MRI, CT and upconversion luminescence tri-modality imaging. Biomaterials. 2012; 33: 4618-4627.

24. Zhao L, Peng J, Huang Q, et al. Near-infrared photoregulated drug release in living tumor tissue via yolk-shell upconversion nanocages. Adv Funct Mater. 2014; 24: 363-371.

25. Lu S, Tu D, Xu J, et al. Multifunctional nano-bioprobes based on rattle-structured upconverting luminescent nanoparticles. Angew Chem Int Edit. 2015; 54: 7915-7919.

26. Wang G, Peng Q, Li Y. Lanthanide-doped nanocrystals: Synthesis, optical-magnetic properties, and applications. Accounts Chem Res. 2011; 44: 322-332.

27. Zivadinov R, Bakshi R. Role of MRI in multiple sclerosis I: Inflammation and lesions. Front Biosci. 2004; 9: 665-683.

28. Generalova AN, Chichkov BN, Khaydukov EV. Multicomponent nanocrystals with anti-Stokes luminescence as contrast agents for modern imaging techniques. Adv Colloid Interfac. 2017; 245: 1-19.

29. Deng M, Wang L. Unexpected luminescence enhancement of upconverting nanocrystals by cation exchange with well retained small particle size. Nano Res. 2014; 7: 782-793.

30. Han S, Deng R, Xie X, et al. Enhancing luminescence in lanthanide-doped upconversion nanoparticles. Angew Chem Int Edit. 2014; 53: 11702-11715.

31. Yang H, Zhuang Y, Sun Y, et al. Targeted dual-contrast T1- and T2-weighted magnetic resonance imaging of tumors using multifunctional gadolinium-labeled superparamagnetic iron oxide nanoparticles. Biomaterials. 2011; 32: 4584-4593.

32. Fan W, Shen B, Bu W, et al. Rattle-structured multifunctional nanotheranostics for synergetic chemo-/radiotherapy and simultaneous magnetic/luminescent dual-mode imaging. J Am Chem Soc. 2013; 135: 6494-6503.

33. Yang X, Xiao Q, Niu C, et al. Multifunctional core-shell upconversion nanoparticles for targeted tumor cells induced by near-infrared light. J Mater Chem B. 2013; 1: 2757-2763.

34. Dai Y, Bi H, Deng X, et al. 808 nm near-infrared light controlled dual-drug release and cancer therapy in vivo by upconversion mesoporous silica nanostructures. J Mater Chem B. 2017; 5: 2086-2095.

35. Han R, Yi H, Shi J, et al. pH-Responsive drug release and NIR-triggered singlet oxygen generation based on a multifunctional core-shell-shell structure. Phys Chem Chem Phys. 2016; 18: 25497-25503.

36. Zhang T, Huang S, Lin H, et al. Enzyme and pH-responsive nanovehicles for intracellular drug release and photodynamic therapy. New J Chem. 2017; 41: 2468-2478.

37. Nguyen TD, Tseng HR, Celestre PC, et al. A reversible molecular valve. 2005; 102: 10029-10034.

38. Bernardos A, Aznar E, Marcos MD, et al. Enzyme-responsive controllerd release using mesoporous silica supports capped with lactose. Angew Chem Int Edit. 2009; 48: 5884-5887.

39. Chen C, Geng J, Pu F, et al. Polyvalent Nucleic acid/mesoporous silica nanoparticles conjugates: Dual stimuli-responsive vehicles for intracellular drug delivery. Angew Chem Int Edit. 2011; 50: 882-886.

40. Sun Y, Feng W, Yang P, et al. The biosafety of lanthanide upconversion nanomaterials. Chem Soc Rev. 2015; 44: 1509-1525.

41. Gnach A, Lipinski T, Bednarkiewicz A, et al. Upconverting nanoparticles: Assessing the toxicity. Chem Soc Rev. 2015; 44: 1561-1584.